Bangladesh J. Plant Taxon. **32**(1): 27–44, 2025 (June) DOI: https://doi.org/10.3329/bjpt.v32i1.82390

COMPLETE CHLOROPLAST GENOME OF *FRAXINUS GRIFFITHII* C.B. CLARKE (OLEACEAE): INSIGHTS INTO GENOME STRUCTURE AND MOLECULAR PHYLOGENETICS

SHEIKH SUNZID AHMED AND M. OLIUR RAHMAN*

Department of Botany, Faculty of Biological Sciences, University of Dhaka, Dhaka 1000, Bangladesh

Keywords: Plastome assembly; Simple sequence repeats; Nucleotide diversity; Phylogenetics; Molecular dating; Oleaceae.

Abstract

This study deciphers the first complete chloroplast (Cp) genome of *Fraxinus griffithii* C.B. Clarke (Oleaceae), a medicinally important tree species native to Bangladesh, providing new insights into its genome structure and phylogenetic relationships. The circular Cp genome comprises a total length of 155,683 bp with a large single-copy region (86,466 bp), small single-copy region (17831 bp), and two inverted repeat regions (51,386 bp). The plastome encodes 130 genes, including 86 protein-coding genes, 36 transfer RNAs and eight ribosomal RNAs. Comparative genomic analysis revealed genome divergence, similar genomic architecture, and lack of large rearrangements within the Oleaceae family. The plastome harbored 46 simple sequence repeats (SSRs) and 49 longer repeats. Among the identified SSRs, mononucleotides (39) were the most frequent, while palindromic repeats predominated among the longer repeats. Nucleotide diversity analysis revealed *rpl32* and *ndhF* genes of the SSC region as the most hypervariable DNA barcodes. Plastome-wide phylogeny supported the systematic position of *F. griffithii* within the subtribe Fraxininae of the tribe Oleeae. Molecular dating analysis suggests that *F. griffithii* originated approximately 15.07 million years ago, during the Langhian stage of the Middle Miocene epoch in the Neogene period of the Cenozoic era. The findings of this study provide the first Cp genome data for *F. griffithii* (GenBank Accession: PP669282.1), contributing to valuable insights into the evolutionary genomics of the family Oleaceae.

Introduction

Fraxinus griffithii C.B. Clarke (family Oleaceae), commonly known as Griffith's ash, is a medicinal tree species native to Bangladesh. The family Oleaceae encompasses numerous ecologically and ethnobotanically significant species, many of which are distributed across temperate and subtropical regions (Huang *et al.*, 2019). *F. griffithii* occurs a wide geographic range, spanning central, eastern, and southeastern Asia, including Bangladesh, Myanmar, China, Vietnam, Taiwan, and Philippines (Macahig *et al.*, 2010). Morphologically, this tree is small to moderate in size, with branchlets varying from pubescent to glabrescent. Leaves are pinnately compound and consist of 5–9 glossy, lanceolate leaflets. The species possesses terminal or axillary panicles of small white flowers, distinctive samaras type of fruits with elongated wings that facilitate wind dispersal (Rahman, 2009). *F. griffithii* demonstrates considerable medicinal potential, supported by both phytochemical and pharmacological evidence. Phytochemical analyses of its leaves have identified 12 bioactive compounds that demonstrated antioxidant properties (Macahig *et al.*, 2010). Beyond its antioxidant capacity, *F. griffithii* has shown central nervous system (CNS)-modulating effects. The traditional use of its bark and leaf extracts in some

*Corresponding author. Email: oliur.bot@du.ac.bd

regions has been linked to sedative properties (Basori, 2004). Phytochemical screening revealing saponins, tannins, and glycosides, often associated with bioactivity highlights the potential of this medicinal tree as a source of neuromodulatory or sedative drug candidates, warranting further therapeutic investigation (Xiao and Bai, 2019).

The chloroplast (Cp) genome serves as an essential tool for taxonomic identification due to its conserved structure, uniparental inheritance, and relatively slow rate of evolution compared to nuclear genomes, making it especially suitable for phylogenetic studies in plants (Dobrogojski *et al.*, 2020). Traditional DNA barcoding typically targets *trnH-psbA*, *matK*, *rbcL*, and *ndhF*, which are effective for species-level identification and widely used in plant systematics (Li *et al.*, 2015). While these markers can provide useful information, however, they often lack sufficient resolution to fully capture the diversity within complex or morphologically variable taxa. In contrast, whole plastome analysis, encompassing all protein-coding genes, tRNAs, and rRNAs, provides a comprehensive genetic dataset that improves species identification accuracy and strengthens phylogenetic inferences (Claude *et al.*, 2025). This complete plastomic approach helps resolve ambiguous species boundaries, uncover cryptic speciation, and clarify evolutionary histories that may be overlooked with partial sequences (Ahmed and Rahman, 2025). Furthermore, when integrated with molecular dating techniques, the complete plastome offers additional advantages by enhancing the statistical robustness of divergence time estimates, enabling more precise calibrations and reducing uncertainty in molecular clock analyses. Such genome-wide data offers deeper insights into lineage diversification, historical biogeography, and key evolutionary events (Zhang *et al.*, 2021a). Therefore, utilizing full Cp genome may offer a strong molecular framework for accurate identification and classification of *F. griffithii* within the broader phylogeny of Oleaceae.

The increasing accessibility of next-generation sequencing (NGS) data has greatly facilitated plastome assembly, annotation and downstream analyses. Repurposing these publicly available datasets enables the assembly of complete plastomes for the first time with high accuracy, while eliminating the cost, and technical demands of new sequencing experiments. This approach further facilitates for broad-scale genomic investigations across a wide range of plant species, even those lacking fresh biological materials. The use of existing data also promotes reproducibility and transparency in research, as raw sequences remain accessible for validation and reanalysis. Moreover, it unlocks new opportunities for comparative genomics, phylogenetic studies, and evolutionary analysis by leveraging the extensive sequence information already deposited in public repositories (Park *et al.*, 2020; Ahmed and Rahman, 2024).

To date, a thorough investigation of the complete plastome of *F. griffithii* has not been conducted, leaving critical gaps in our understanding of its systematic placement and evolutionary history across geological timescales. In this study, we aim to construct and analyze the complete plastome of *F. griffithii* for the first time, integrating phylogenetic reconstruction and molecular dating analyses. The resulting insights are expected to refine its genetic classification, illuminate its evolutionary trajectory, and support conservation strategies, while also providing a valuable genomic resource for further studies on its ecological relevance.

Materials and Methods

NGS reads acquisition and quality control

The Illumina reads **(**SRR28778062**)** of *F. griffithii* were retrieved from the NCBI Sequence Read Archive (SRA) database. The Illumina HiSeq X platform generated approximately 19.1 million reads, yielding 5.7 Gb of bases with a total data size of 2.1 Gb. The sequencing library (BOP132327) followed a paired-end approach with size fractionation for optimal coverage. Data

quality was verified using FASTQC v.0.12.1 to confirm read reliability prior to downstream analysis (Ahmed and Rahman, 2024).

Assembly, annotation and NCBI submission

The complete plastome was assembled from Illumina sequencing reads employing the GetOrganelle tool v1.7.7.0 (Jin *et al.*, 2000). Coverage depth was assessed through UGENE, and gene annotation was performed with the CPGAVAS2 platform, and further cross-checked by CPGView server (Okonechnikov *et al.*, 2012; Shi *et al.*, 2019; Liu *et al.*, 2023). The annotated plastome was visualized via the Chloroplot web-tool (Zheng *et al.*, 2020). The finalized organellar genome sequence has been submitted to the NCBI GenBank database with the accession number "PP669282.1".

Repeats and codon usage analysis

Simple Sequence Repeats (SSRs) present in the plastome were detected with the MISA-Web tool under default parameters, while long repeat elements were identified using the REPuter server, considering all possible matching orientations (Kurtz *et al.*, 2001; Beier *et al.*, 2017). Codon usage bias was analyzed with the RSCU (Relative Synonymous Codon Usage) module in MEGA v.11 (Tamura *et al.*, 2021). The codon usage data were subsequently visualized as a heatmap generated via a Python script utilizing the pandas, seaborn, and matplotlib libraries.

Contraction and expansion of IR

Structural changes of Inverted Repeat (IR) regions in *F. griffithii* were examined using the IRscope web-tool (Amiryousefi *et al.*, 2018). The annotated GenBank file was uploaded alongside plastome annotation files from closely related species to enable comparative analysis of the junction sites. Following the generation of the visualization plot, the output was downloaded and analyzed to assess structural deviations in the IR margins and the orientation of adjacent genes.

Comparative genomics and collinearity study

Comparative genomic analysis of the assembled plastome was carried out using the mVISTA platform to evaluate sequence conservation across related species (Frazer *et al.*, 2004). To investigate gene order and structural rearrangements, progressive alignment was carried out via Mauve v.20150226 (Darling *et al.*, 2004). Additionally, collinearity relationships within the plastome were explored using the Circoletto server, applying default parameters for visualization (Darzentas, 2010).

Nucleotide diversity evaluation

The Cp genomes of closely related taxa including *F. grifithii* were aligned with the MAFFT tool (Katoh and Standley, 2013). Following the alignment, nucleotide diversity was calculated using DnaSP v.5 to enable a comprehensive assessment of variability throughout the Cp genomes (Librado and Rozas, 2009).

Molecular phylogenetic and dating assessments

Phylogenetic relationships were assessed in MEGA v.11 employing the Neighbor-Joining (NJ) method (Tamura *et al.*, 2021). For molecular dating, the RelTime-ML submodule was utilized. The analysis was initiated by importing the aligned plastome sequences, and divergence times were estimated using calibration nodes from the TimeTree server (Kumar *et al.*, 2017).

Results and Discussion

Plastome assembly and annotation

The assembled plastome of *F. griffithii* had a total length of 155,683 bp and displayed the typical quadripartite arrangement characteristic of most angiosperms. It comprised a LSC zone of 86,466 bp, a SSC zone of 17,831 bp, and two identical IR zones, each measuring 25,693 bp (Fig. 1). The nucleotide composition of the plastome revealed an overall AT-rich pattern, with 62.14% AT content and 37.86% GC content (Table 1).

Table 1. Nucleotide arrangements of the plastome of *F. griffithii.*

Area	C (%)	G (%)	A (%)	T (U) (%)	C + G (%)	A + T (%)
SSC	15.03	17.02	33.95	34.00	32.05	67.95
LSC	18.36	17.53	31.51	32.60	35.89	64.11
IRA	20.83	22.38	28.53	28.26	43.21	56.79
IRB	22.38	20.83	28.26	28.53	43.21	56.79
Plastome	19.05	18.81	30.76	31.38	37.86	62.14

The SSC demonstrated the highest AT content (67.95%), followed by the LSC (64.11%), whereas both inverted repeats (IRa and IRb) showed lower AT content (56.79%) and comparatively higher GC content (43.21%). IRs depicted higher GC content which is a characteristic feature of angiosperm plastome and carries important biological significance. GC enriched region contributes to greater thermodynamic stability of DNA, enhancing the structural integrity of the IR regions. This stability is particularly important as the IRs often contain functionally essential and highly conserved genes, such as ribosomal RNAs (rRNAs) and some transfer RNAs (tRNAs), which are essential for plastid gene expression as well as ribosomal function. Moreover, the conserved nature and increased GC content of the IRs may play a protective role against large-scale genomic rearrangements, thereby maintaining plastome organization and ensuring evolutionary conservation across plant lineages. These variations in base composition across different regions are consistent with the established trends and reflect the conserved yet region-specific nucleotide distribution within the chloroplast genome (Ahmed and Rahman, 2024, 2025).

The coverage analysis of the *F. griffithii* plastome revealed a high sequencing depth across the genome, ensuring reliable base calling and assembly accuracy. The maximum coverage was recorded at position 121,635, reaching 2,531X, while the minimum coverage occurred at position 12,735, with a depth of 302X (Fig. 2). The mean coverage across the entire plastome was 1,824.8X, indicating a robust and uniform sequencing effort. This high average depth not only validates high genomic integrity but also minimizes the likelihood of sequencing errors, thereby enhancing the reliability of downstream analyses, such as gene annotation, phylogenetics, and molecular dating. When compared to the plastome of *Scaphium scaphigerum*, which exhibited a mean coverage of 990.165X, with a coverage ranging from 14X (min.) to 1,350X (max.), the *F. griffithii* plastome demonstrated substantially higher and more consistent sequencing depth (Ahmed and Rahman, 2025). Notably, the minimum coverage in *F. griffithii* (302X) was significantly higher than that of *S. scaphigerum* (14X), suggesting greater uniformity across the genome. Additionally, the higher peak coverage in *F. griffithii* further reinforces confidence in base accuracy, particularly in regions critical for functional annotation and comparative genomic analyses.

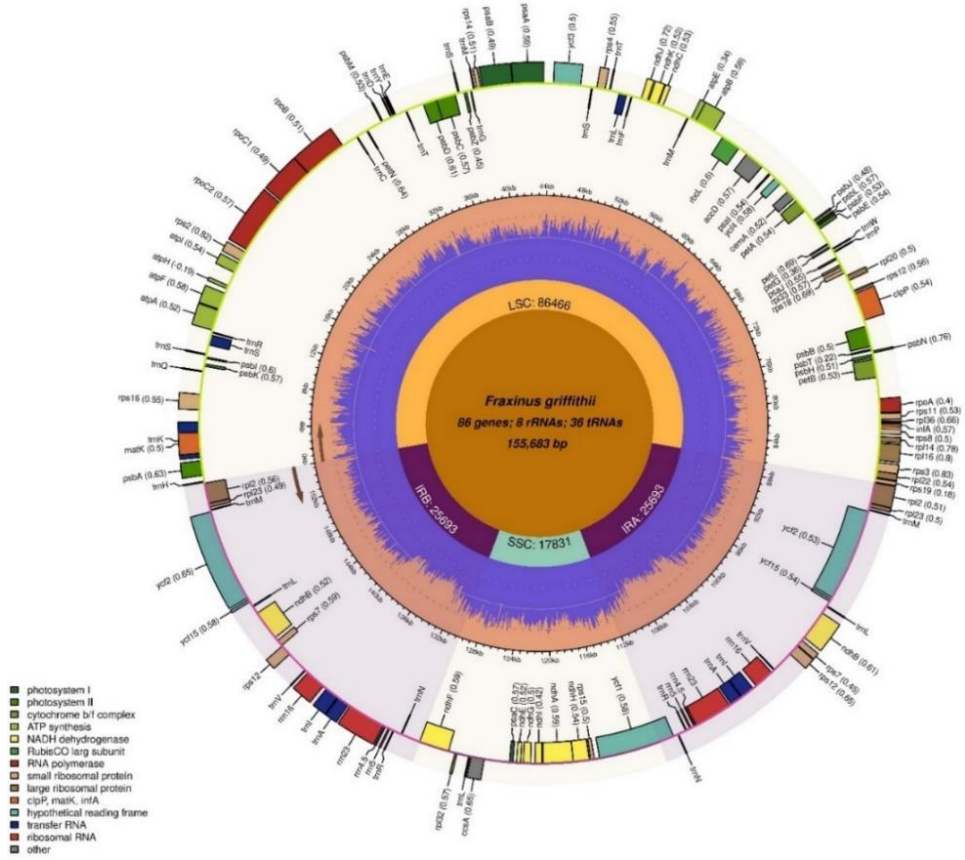

Fig. 1. Orbicular plastome map of *F. griffithii* illustrating quadripartite junction sites and their gene contents.

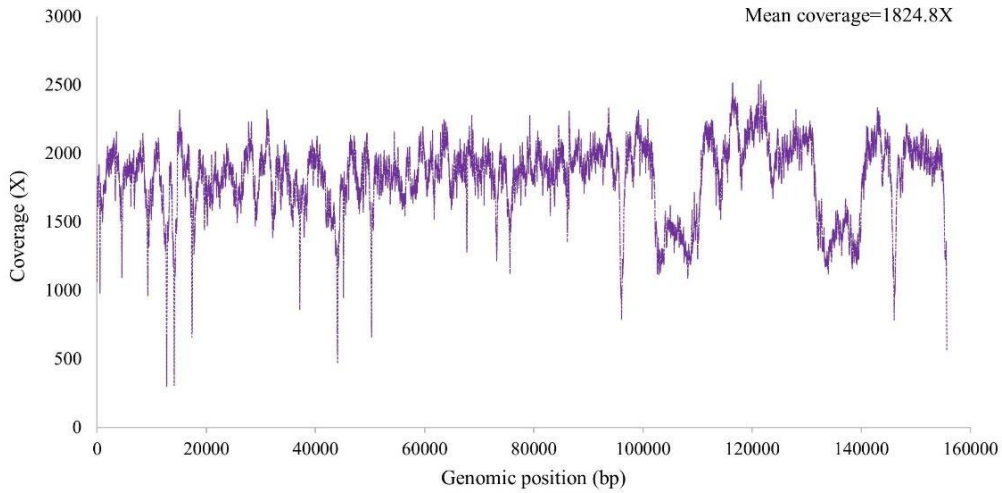

Fig. 2. Coverage depth assessment of the complete Cp genome of *F. griffithii* elucidating robust base accuracy and high quality of the assembled plastome.

The genome annotation of the *F. griffithii* plastome identified 130 functional genes, comprising 86 protein-coding genes (PCGs), 36 tRNAs, and eight rRNAs. These genes were functionally grouped into categories related to photosynthesis, self-replication, and other essential plastid functions. Key genes for photosynthesis included those encoding subunits of ATP synthase, photosystems I and II, NADH-dehydrogenase, cytochrome b/f complex, and rubisco enzyme (Table 2). Genes involved in self-replication comprised large and small ribosomal subunits, and RNA polymerases. Additional genes encoded proteins such as maturase (*matK*), protease (*clpP*), and various conserved hypothetical reading frames (*ycf* genes), reflecting the structural and functional completeness of the annotated plastome.

Table 2. Protein-coding genes in the plastome of *F. griffithii.*

Category	Group	Name of genes
Genes for photosynthesis	Subunits of ATP synthase	*atpA, atpB, atpE, atpF, atpH, atpI*
	Subunits of photosystem II	*psbA, psbB, psbC, psbD, psbE, psbF, psbH, psbI, psbJ, psbK, psbL, psbM, psbN, psbT, psbZ*
	Subunits of NADH-dehydrogenase	*ndhA, ndhB* (×2), *ndhC, ndhE, ndhF, ndhG, ndhH, ndhI, ndhJ, ndhK*
	Subunits of cytochrome b/f complex	*petA, petB, petG, petL, petN*
	Subunits of photosystem I	*psaA, psaB, psaC, psaI, psaJ*
	Subunit of rubisco	*rbcL*
Self-replication	Large subunit of ribosome	*rpl14, rpl16, rpl2* (×2), *rpl20, rpl22, rpl23* (×2), *rpl32, rpl33, rpl36*
	DNA dependent RNA polymerase	*rpoA, rpoB, rpoC1, rpoC2*
	Small subunit of ribosome	*rps2, rps3, rps4, rps7* (×2), *rps8, rps11,* rps12 (×3), rps14, *rps15, rps16, rps18, rps19*
Other genes	Subunit of Acetyl-CoA-carboxylase	*accD*
	c-type ytochrome synthesis gene	*ccsA*
	Envelop membrane protein	*cemA*
	Protease	*clpP*
	Translational initiation factor	*infA*
	Maturase	*matK*
Unknown	Conserved open reading frames	*ycf1, ycf2* (×2), *ycf3, ycf4, ycf15* (×2)

F. griffithii chloroplast genome uncovered the presence of several cis-splicing genes, each characterized by distinct exon-intron structures that support precise post-transcriptional modification processes within the plastid (Fig. 3). The accurate identification of intron-containing genes with defined splice sites confirms the structural completeness of the annotated plastome as well as highlights the complexity of chloroplast gene regulation, which is essential for maintaining organelle functionality and plant development. Figure 4 illustrates the trans-splicing arrangement of the *rps12* gene within the plastome. In this configuration, exon1 of *rps12* is encoded on the negative strand within the LSC, while the other two exons are duplicated and situated in the IRs (IRa and Irb) on opposite strands. Two distinct mature transcripts are formed through trans-splicing: one joining exon1 with exons 2 and 3 from IRa, and another with exons 2 and 3 from

IRb. This structure highlights the unique gene architecture of *rps12* and its reliance on trans-splicing to generate functional transcripts from spatially separated genomic regions.

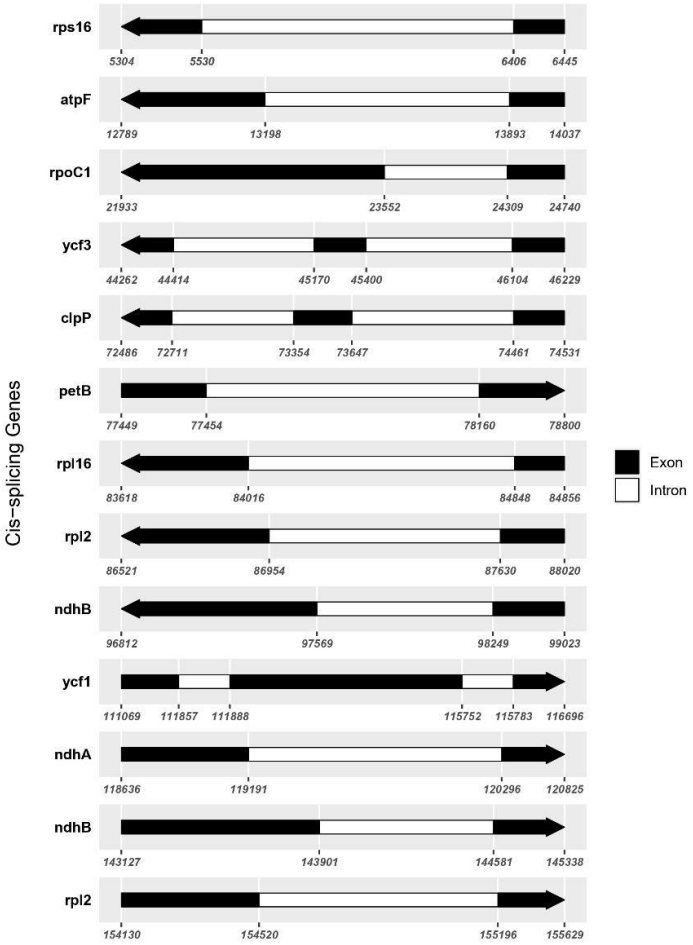

Fig. 3. Schematic representation of the genes involved in the cis-splicing process of the Cp genome of *F. griffithii.*

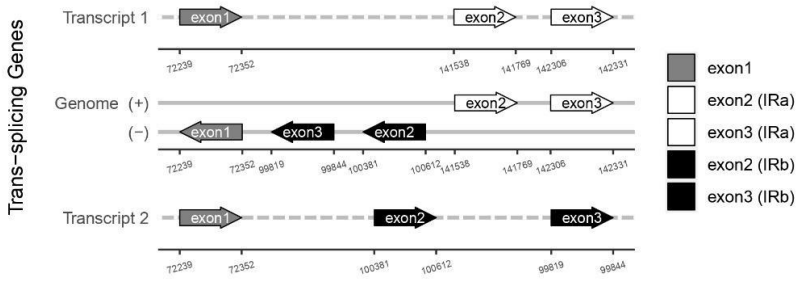

Fig. 4. Schematic representation of the gene *rps12* involved in the trans-splicing process of the Cp genome of *F. griffithii.*

Repeats and codon usage pattern

The SSR analysis of *F. griffithii* and related *Fraxinus* species revealed varying distributions of simple sequence repeats (SSRs). *F. griffithii* contained 46 SSRs, predominantly mononucleotide repeats (39), followed by di- (3), tetra- (3), and one pentanucleotide repeat (Fig. 5A). Among other species, *F. chinensis* exhibited the highest number (60) of SSRs with 48 mononucleotide, seven dinucleotide, one trinucleotide and four tetranucleotide repeats. *F. griffithii* depicted close similarity in SSR contents with *F. malacophylla* and *F. velutina*, both of which showed 50 SSRs in total. The variation in SSR number and motif types across species highlights species-specific patterns that can reveal useful phylogenetic markers for evolutionary studies, population genetics, and conservation planning. In particular, the relatively conserved SSR profile observed in *F. griffithii*, *F. malacophylla*, and *F. velutina* suggests a degree of evolutionary closeness, while the higher SSR diversity in *F. chinensis* may indicate greater plastome variability (Wu *et al.*, 2018). The REPuter server identified 49 longer repeat structures in the plastome of *F. griffithii* comprising 16 forward, 11 reverse, 21 palindromic, and one complement repeat (Fig. 5B). Among these, palindromic sequences were the most frequent, followed by forward repeats. The presence of these repetitive elements may contribute to genome stabilization, structural variation, and plastome evolution. Notably, the overall repeat pattern in *F. griffithii* showed a degree of similarity to other *Fraxinus* species, supporting the accuracy and correctness of the plastome assembly. This concordance suggests that the assembly reflects genuine biological features rather than technical artifacts, thereby reinforcing confidence in subsequent analyses (Albediwi *et al.*, 2024).

Fig. 5. Comparative assessment of repeat structures in *F. griffithii* and its closely related taxa. A. Simple sequence repeats, B. Longer repeats.

The codon usage analysis of the *F. griffithii* plastome revealed diversity in the RSCU scores among the 64 codons (Fig. 6). The highest RSCU value was observed for AGA (arginine) at 1.94, indicating a strong preference for this codon, while the lowest was for CGC (arginine) at 0.51, suggesting the weakest preference. Codons such as AUG (methionine) and UGG (tryptophan) showed an RSCU value of 1, reflecting their roles as single codons without synonymous alternatives. This pattern was consistent with related *Fraxinus* species, all showing a preference for AGA and reduced usage of CGC, highlighting a conserved codon usage bias across the genus. These findings may reflect translational efficiency and evolutionary adaptation in the plastid genomes of *Fraxinus* species.

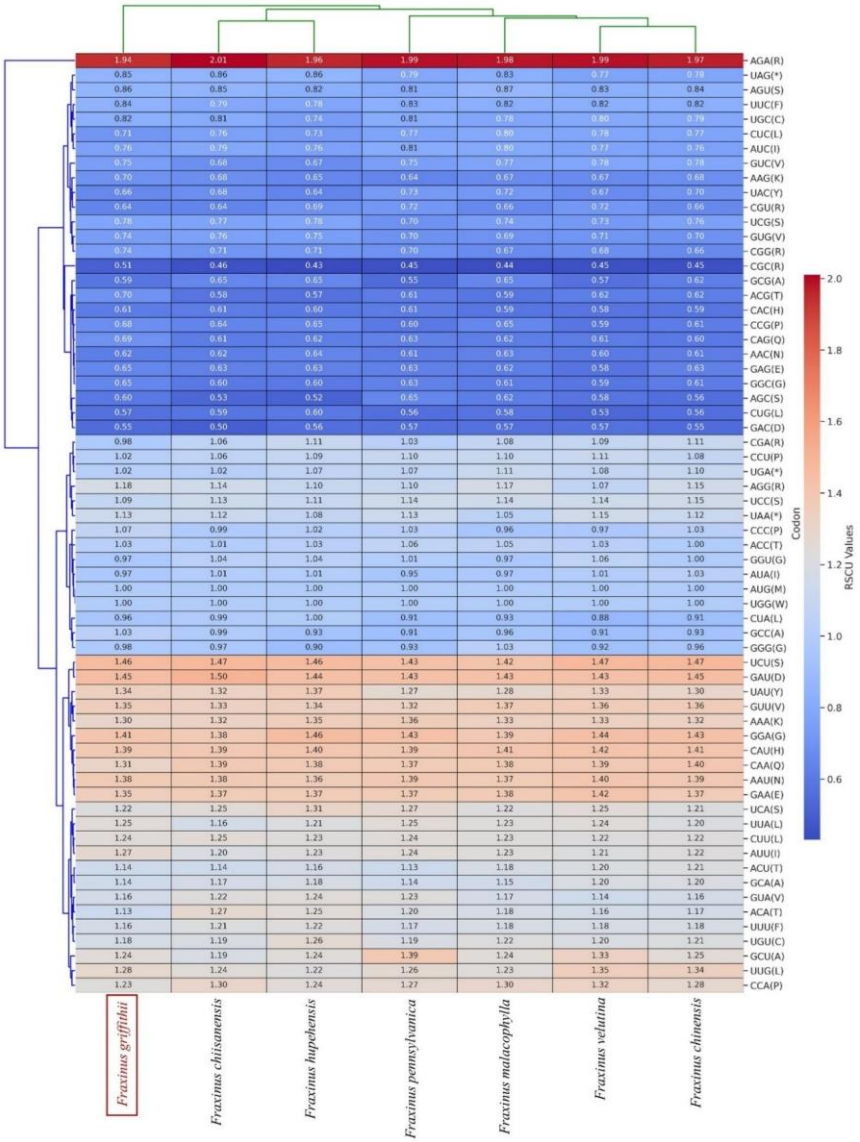

Fig. 6. Heatmap illustrating codon usage pattern of *F. griffithii* and closely related species.

IR expansion and contraction

The size of the LSC varied from 86,389 to 86,696 bp, while the SSC ranged between 17,760 and 19,109 bp across the examined taxa (Fig. 7). In comparison to *Syringa villosa*, a minor expansion of the IRs was observed in *F. griffithii* and other *Fraxinus* species, suggesting localized shifts in boundary positioning. Conversely, when compared to *Olea europaea* and *Comoranthus minor*, the IR regions *in F. griffithii* exhibited mild contraction. These junctional changes typically involved genes such as *rps19* and *ycf1*, which are often located at or near the IR boundaries. The observed stability and modest variation in IR boundaries within *Fraxinus* support the structural integrity of the assembled plastome and reflect evolutionary constraints acting on the chloroplast genome. Expansions or contractions of IRs may influence plastome size and have implications for phylogenetic inference and genome evolution (Guo *et al.*, 2021).

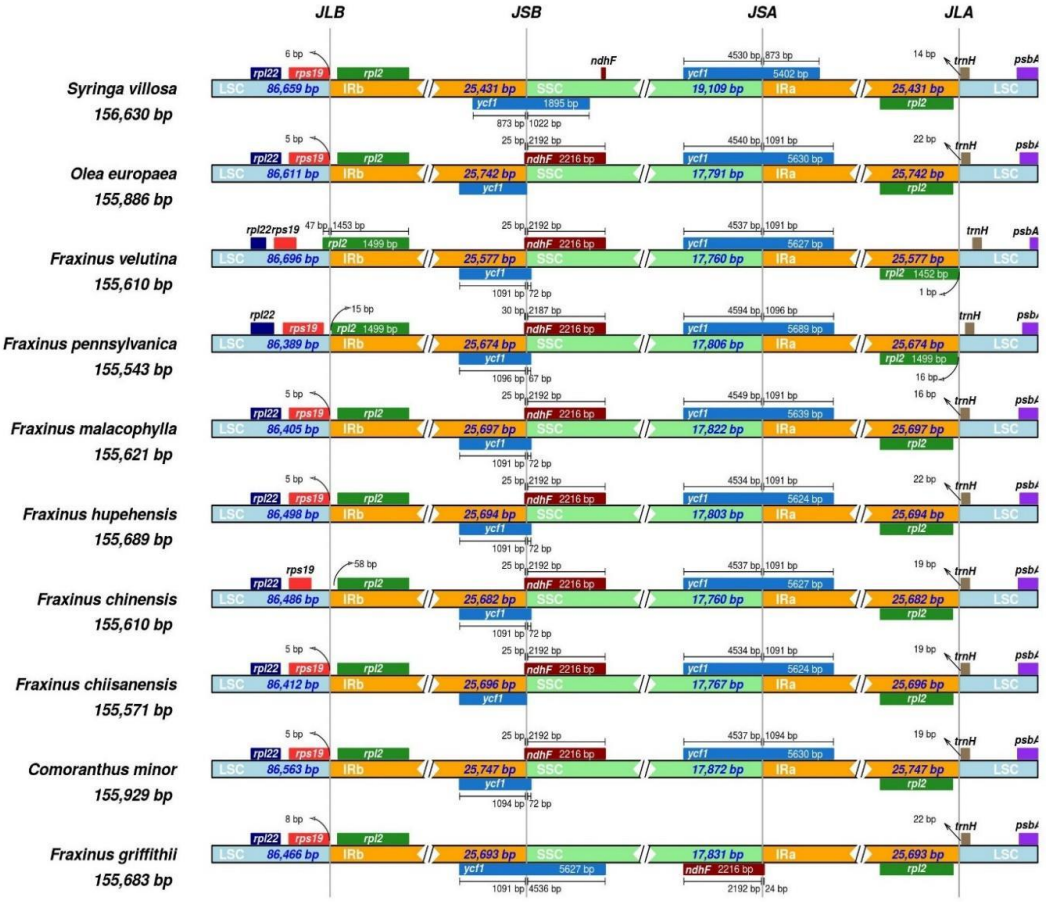

Fig. 7. LSC, SSC, and IR regions in the *F. griffithii* and related plastomes illustrating quadripartite junction sites. Numbers displayed above or beside the color-coded genes indicate the distances from each gene to the adjacent junctions.

Comparative genomics and collinearity

The genome divergence study with *F. griffithii* as the reference, revealed notable sequence variation primarily focused in the single-copy regions, while the IRs remained relatively

conserved across all examined taxa (Fig. 8). Among the aligned genomes, most variations were detected in intergenic spacers and intronic parts of the LSC and SSC, whereas gene-coding sequences showed a high level of conservation, reflecting their functional constraints. This pattern of variation is consistent with established trends in angiosperm plastome and underscores the stabilizing influence of the IR regions. The observed divergence in single-copy regions highlights their potential utility for developing species-specific molecular markers, facilitating phylogenetic reconstruction, and resolving taxonomic ambiguities within the genus (Ferguson, 2002), and our results are supported by previous findings (Zhang *et al.*, 2021b; Albediwi *et al.*, 2024).

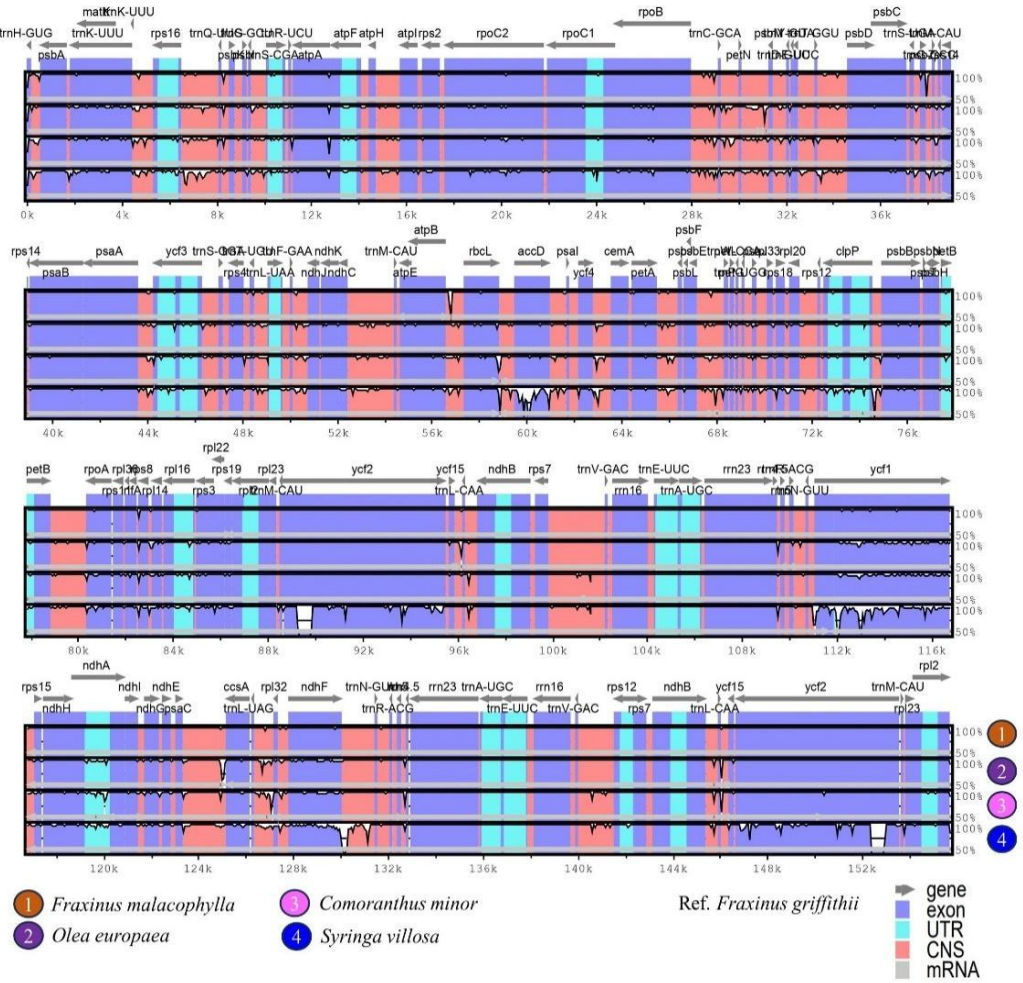

Fig. 8. Genome divergence analysis elucidating gene orders, variations and conservation across all the plastome compartments of *F. malacophylla*, *Olea europaea*, *Comoranthus minor* and *Syringa villosa*, using *F. griffithii* as the reference genome.

The progressive Mauve alignment revealed highly similar locally collinear blocks (LCBs) across the compared plastomes, indicating strong conservation of genomic structure among *F. griffithii* and its closely related species (Fig. 9). Gene order and arrangement were visualized

through multicolored blocks, with red representing rRNA genes, black for tRNAs, green for intron-containing tRNAs, and white for protein-coding genes (PCGs). The absence of major structural rearrangements or inversions further supports the structural integrity of the *F. griffithii* plastome. This high degree of synteny not only confirms the accuracy of the genome assembly and annotation but also reflects the evolutionary stability of plastid genomes within the genus, providing a reliable basis for phylogenetic and comparative genomic studies. Our results are supported by previous findings based on Mauve progressive alignments (Alsuhaimi *et al.*, 2024; Ahmed and Rahman, 2025).

Fig. 9. Comparative genomics analysis showing genome-wide collinearity and similar arrangement of the genomic compartments across various plastomes. A. *Fraxinus griffithii*, B. *F. chiisanensis*, C. *F. chinensis*, D. *F. hupehensis*, E. *F. malacophylla*, F. *pennsylvanica*, and G. *F. velutina*.

Synteny analysis using the Circoletto server effectively visualized the conserved genomic blocks between *F. griffithii* and its close relatives, highlighting substantial levels of sequence similarity and structural conservation (Fig. 10). The circular representation revealed strong syntenic relationships, particularly in coding regions, illustrated by well-aligned, colored ribbons connecting homologous loci among the compared plastomes. These conserved syntenic blocks indicate limited genomic rearrangements, underscoring the evolutionary stability of chloroplast genomes within the genus *Fraxinus*. The findings align well with previous reports (Alsuhaimi *et al.*, 2024; Ahmed and Rahman, 2025). The present study revealed the key genomic features of species closely related to *Fraxinus griffithii*, including the highest GC content in *Ligustrum lucidum*, the highest number of protein-coding genes in *Fraxinus pennsylvanica*, and the highest number of tRNAs in *Osmanthus cooperi* (Table 3).

Employing multiple tools in the present study such as mVISTA, Mauve, and Circoletto, ensured a robust and multidimensional validation of the genomic features and evolutionary relationships of the *F. griffithii* plastome. Each tool offers unique analytical strengths: mVISTA enables fine-scale visualization of sequence divergence across entire plastomes, highlighting variation in coding and non-coding regions (Frazer *et al.*, 2004); Mauve identifies locally collinear blocks, revealing structural rearrangements and gene order conservation (Darling *et al.*, 2004); while Circoletto graphically presents synteny and homology across species in an intuitive circular

format (Darzentas, 2010). The complementary nature of these platforms enhances analytical reliability by cross-validating genomic patterns from multiple perspectives. This integrated approach not only reinforces confidence in the assembly and annotation of the *F. griffithii* plastome but also provides deeper insights into its structural conservation and evolutionary dynamics within the Oleaceae family. The utility of this multi-dimensional approach is further supported by similar studies (Alsuhaimi *et al.*, 2024; Ahmed and Rahman, 2025).

Table 3. Comparative overview of Cp genomes within the family Oleaceae.

Taxa	Accessions	Tribe	Plastome (bp)	GC (%)	PCGs	rRNAs	tRNAs	Total Genes
Abeliophyllum distichum	MN127986.1	Forsythieae	156,008	37.82	89	8	37	134
Chionanthus retusus	NC_035000.1	Oleeae	155,687	37.76	89	8	37	134
Chrysojasminum fruticans	MH559274.1	Jasmineae	159,404	37.45	88	8	38	134
Comoranthus minor	MH817901.1	Oleeae	155,929	37.79	89	8	35	132
Fontanesia phillireaeoides subsp. fortunei	MG255754.1	Fontanesieae	155,992	37.74	88	8	35	131
Forsythia mira	NC_046065.1	Forsythieae	156,485	37.80	89	8	37	134
Forsythia suspensa	NC_036367.1	Forsythieae	156,404	37.79	89	8	37	134
Fraxinus chiisanensis	MF980720.1	Oleeae	155,571	37.89	89	8	37	134
Fraxinus chinensis	MW599993.1	Oleeae	155,610	37.84	89	8	35	132
Fraxinus griffithii	PP669282.1	Oleeae	155,683	37.86	86	8	36	130
Fraxinus hupehensis	NC_052770.1	Oleeae	155,689	37.85	89	8	35	132
Fraxinus malacophylla	MT663306.1	Oleeae	155,621	37.86	88	8	35	131
Fraxinus pennsylvanica	NC_043874.1	Oleeae	155,543	37.84	92	8	36	136
Fraxinus velutina	NC_082971.1	Oleeae	155,610	37.84	90	8	35	133
Jasminum sambac	MN158204.1	Jasmineae	163,315	37.52	89	8	37	134
Ligustrum lucidum	MH394207.1	Oleeae	154,793	38.24	83	8	35	126
Myxopyrum hainanense	NC_047485.1	Myxopyreae	156,064	37.72	86	8	37	131
Nestegis sandwicensis	NC_042457.1	Oleeae	155,565	37.77	89	8	35	132
Nyctanthes arbor-tristis	PP055962.1	Myxopyreae	155,567	37.74	86	8	33	127
Olea europaea	MT182986.1	Oleeae	155,886	37.81	89	8	37	134
Osmanthus cooperi	NC_053565.1	Oleeae	155,262	37.80	82	8	44	134
Schrebera trichoclada	NC_042268.1	Oleeae	155,644	37.80	89	8	35	132
Syringa villosa	OL414766.1	Oleeae	156,630	37.97	88	8	37	133

Nucleotide diversity

F. griffithii plastome revealed an average diversity (π) value of 0.025334, indicating a moderate level of genetic variation across the genome (Fig. 11). The highest nucleotide diversity was observed in the *rpl32* (π = 0.11149), followed by *ndhF* (π = 0.11062), both positioned in the SSC, suggesting this portion harbors the most divergent loci. Within the LSC, the *accD* (π = 0.08432) and *trnF* (π = 0.06291) showed the highest levels of variability. In contrast, the IRa and IRb regions exhibited relatively low nucleotide diversity, reflecting their conserved nature. These findings indicate that the SSC and LSC regions contain more polymorphic sites, which may be valuable for molecular evolutionary analysis and the development of phylogenetic markers in *Fraxinus* and its closely related species (Alsuhaimi *et al.*, 2024).

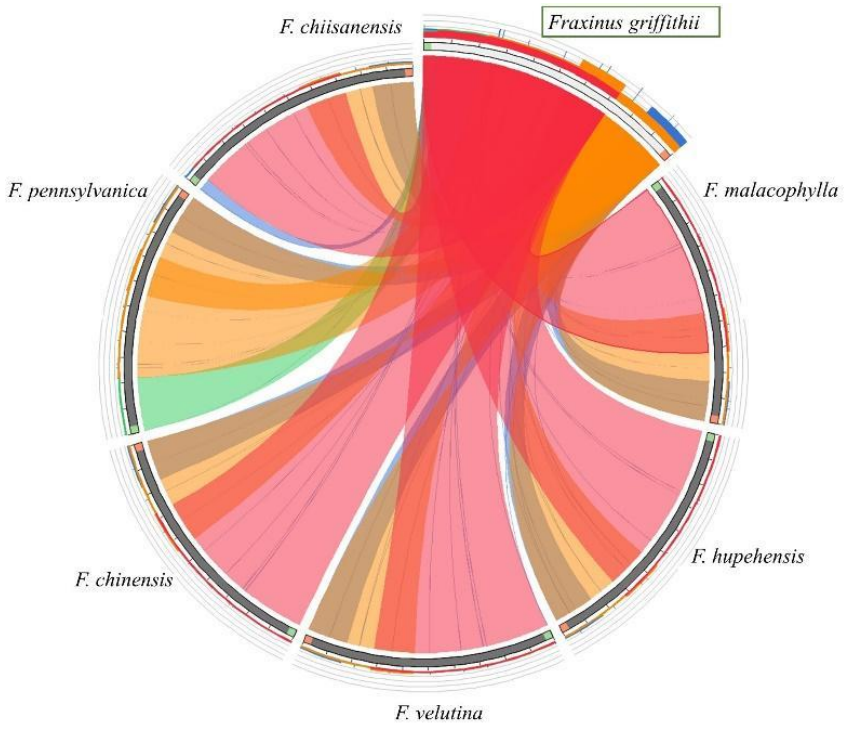

Fig. 10. Comparative genomic analysis showing syntenic blocks between *F. griffithii* and other closely related members within the Oleaceae.

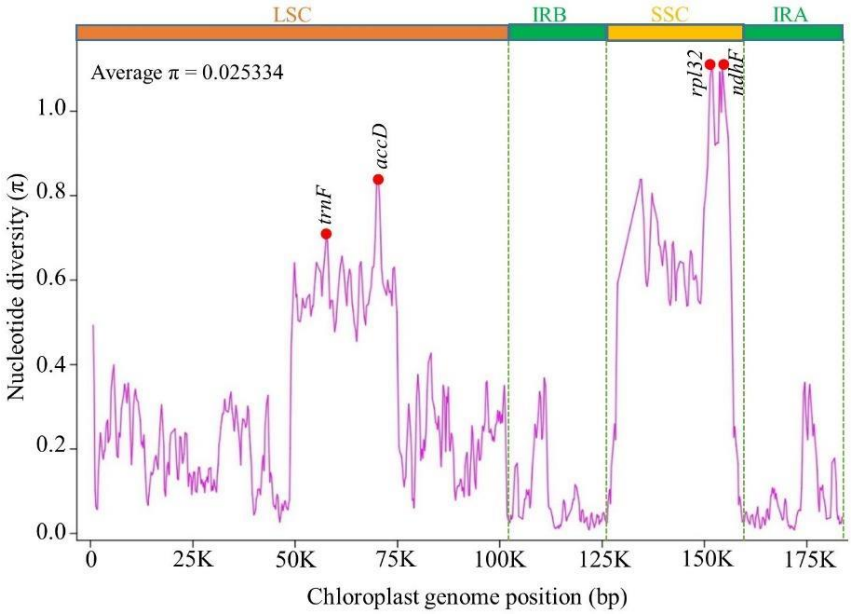

Fig. 11. Nucleotide diversity assessment of the *F. griffithii* plastome annotating hypervariable DNA barcodes.

Molecular phylogenetic and dating endeavor

The NJ (Neighbor-Joining) tree supported the assembly of *F. griffithii* by showing its clustering with other closely related members of the same genus within the subtribe Fraxininae of the tribe Oleeae (Fig. 12). *F. griffithii* showed a closer relationship with *F. malacophylla* than with other *Fraxinus* members. Within the tribe Oleeae, the subtribe Fraxinninae exhibited a close affinity with the subtribe Oleinae. All four subtribes of Oleeae depicted monophyletic origins, with nearly 100% bootstrap support, underscoring the robustness of the phylogenetic tree. Similarly, members of the other four tribes, such as Fontanesieae, Forsythieae, Jasmineae, and Myxopyreae also showed monophyly. The phylogeny of the members was congruent with earlier reports based on complete chloroplast genomes of *F. pennsylvanica* and *F. malacophylla* (Yi *et al.*, 2019; Duan *et al.*, 2020).

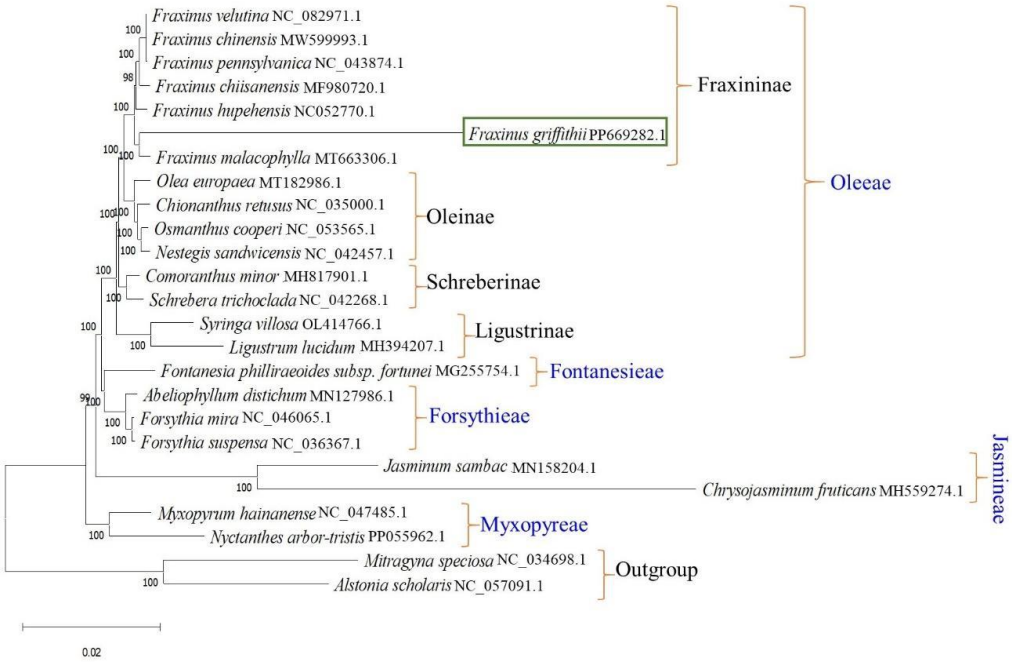

Fig. 12. Neighbor-joining tree illustrating plastome-wide phylogenetic affinities of *F. griffithii* within the family Oleaceae.

Molecular dating analysis revealed the earliest divergence within the Oleaceae occurred approximately 56.50 million years ago (MYA) during the Thanetian age of the late Paleocene epoch in the Paleogene period of the Cenozoic era (Fig. 13). The *Fraxinus* clade diverged around 17.14 MYA, during the Burdigalian age of the early Miocene epoch in the Neogene period. *F. griffithii* showed a divergence time of approximately 15.07 MYA, corresponding to the Langhian age of the Middle Miocene epoch in the Neogene period. These estimates, derived from complete plastome sequences, provide robust temporal framework for understanding evolutionary events, and offer valuable insights into lineage diversification and historical biogeography within the Oleaceae. The application of plastome-wide molecular dating is further supported by its consistency with findings from previous studies (Zhang *et al.*, 2021a; Ahmed and Rahman, 2024, 2025).

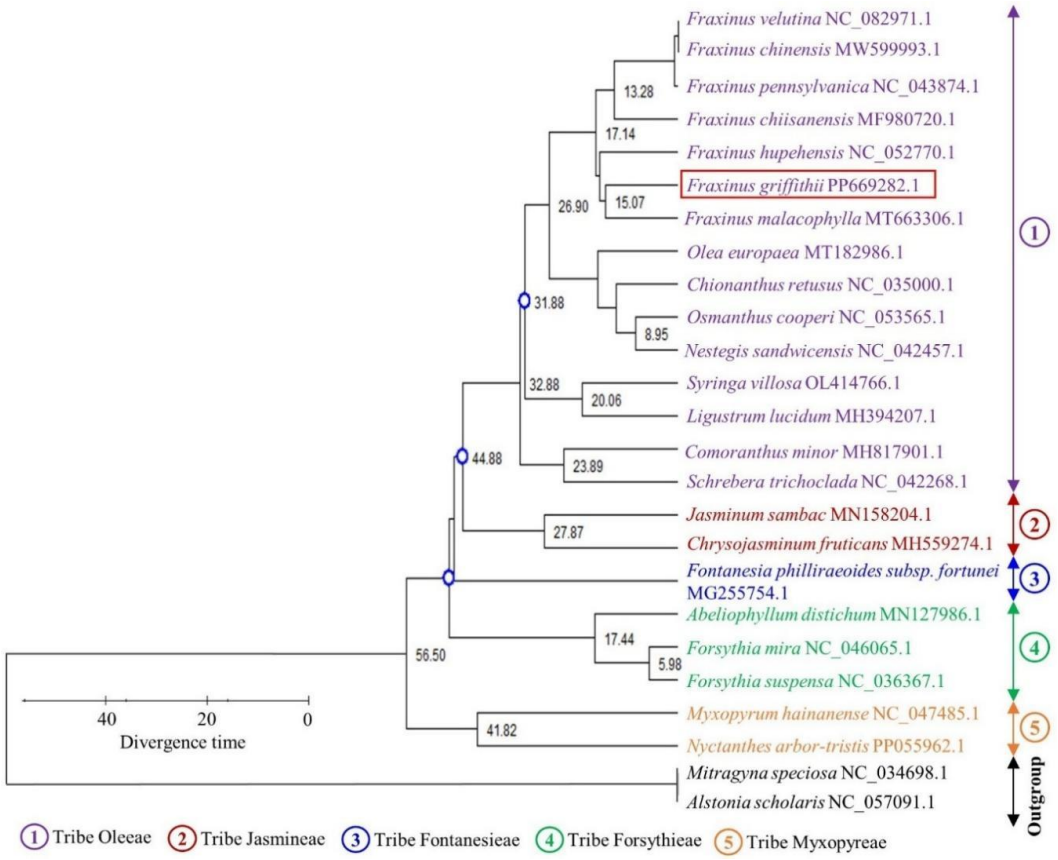

Fig. 13. Molecular dating analysis elucidating species divergence in million years ago (MYA) within the family Oleaceae.

In this investigation, we report the first complete chloroplast genome sequence of *Fraxinus griffithii* (GenBank Accession: PP669282.1), thereby filling a significant gap in the plastome data for the genus *Fraxinus*. Comprehensive analyses, including genome assembly, annotation, repeat structure, and codon usage profiling, have provided critical insights into the structural and functional features of the *F. griffithii* plastome. Comparative plastomic analyses with related species revealed a conserved genome organization, identified variation hotspots, and uncovered key evolutionary patterns. Nucleotide diversity assessment underscored highly variable loci, offering promising targets for future phylogeographic and population-level studies. Phylogenetic reconstruction and molecular dating based on full plastome sequences established robust evolutionary relationships and divergence timelines within the Oleaceae. Collectively, this investigation provides a valuable genomic resource for *F. griffithii* and contributes to a deeper perception of plastome evolution, systematics, and biogeography within the Oleaceae family.

References

Ahmed, S.S. and Rahman, M.O. 2024. Deciphering the complete chloroplast genome sequence of *Meconopsis torquata* Prain: Insights into genome structure, comparative analysis and phylogenetic relationship. Heliyon **10**: e36204.

Ahmed, S.S. and Rahman, M.O. 2025. Comparative genomics and phylogenetic analysis of complete chloroplast genome of *Scaphium scaphigerum* (Wall. *ex* G. Don) G. Planch. Dhaka Univ. J. Biol. Sci. **34**(1): 119–143.

Albediwi, A.S., Ali, M.A., Alwahibi, M.S., Ahmed, S.S., Rahman, M.O., Kim, S.Y., Elshikh, M.S. and Alsuhaimi, N.M. 2024. Unveiling the complete chloroplast genome of *Tribulus macropterus* var. *arabicus* (Hosni) Al-Hemaid & J. Thomas: Genome structure, comparative analysis and phylogeny. Bangladesh J. Plant Taxon. **31**(1): 1–14.

Alsuhaimi, N.M., Ali, M.A., Alwahibi, M.S., Ahmed, S.S., Rahman, M.O., Pandey, S.K., Elshikh, M.S., Alshallali, S.R.S., Lee, J. and Kim, S.Y. 2024. Complete chloroplast genome sequence of a novel *Withania somnifera* (L.) Dunal: Comparative genomics and phylogenetic insights. Bangladesh J. Plant Taxon. **31**(2): 205–223.

Amiryousefi, A., Hyvönen, J. and Poczai, P. 2018. IRscope: An online program to visualize the junction sites of chloroplast genomes. Bioinform. **34**(17): 3030–3031.

Basori, A. 2004. Pharmacodynamic identification of antiseizure effect of ligustrosid glycoside (a CNS active substance) isolated from *Fraxinus griffithii* clarke on mice. Folia Med. Indon. **40**(3): 103-107.

Beier, S., Thiel, T., Münch, T., Scholz, U. and Mascher, M. 2017. MISA-web: A web server for microsatellite prediction. Bioinform. **33**(16): 2583–2585.

Claude, S.J., Kamra, K., Jung, J., Kim, H.O. and Kim, J.H. 2025. Elucidating the evolutionary dynamics of parasitism in *Cuscuta*: in-depth phylogenetic reconstruction and extensive plastomes reduction. BMC Genomics **26**(1): 1–13.

Darling, A.C., Mau, B., Blattner, F.R. and Perna, N.T. 2004. Mauve: Multiple alignment of conserved genomic sequence with rearrangements. Genome Res. **14**(7): 1394–1403.

Darzentas, N. 2010. Circoletto: Visualizing sequence similarity with Circos. Bioinform. **26**(20): p2620.

Dobrogojski, J., Adamiec, M. and Luciński, R. 2020. The chloroplast genome: A review. Acta Physiol. Plant. **42**(6): 98.

Duan, H.C., Zheng, X.H., Li, Y.Y., Li, S.M., Ye, L., Jing, H.Z. and Dong, Q. 2020. The complete chloroplast genome of *Fraxinus malacophylla* (Oleaceae, Oleoideae). Mitochon. DNA Part B. **5**(3): 3570–3571.

Ferguson, J.W.H. 2002. On the use of genetic divergence for identifying species. Biol. J. Linn. Soc. **75**(4): 509–516.

Frazer, K.A., Pachter, L., Poliakov, A., Rubin, E.M. and Dubchak, I. 2004. VISTA: Computational tools for comparative genomics. Nucleic Acids Res. **32**: W273–W279.

Guo, Y.Y., Yang, J.X., Bai, M.Z., Zhang, G.Q. and Liu, Z.J. 2021. The chloroplast genome evolution of Venus slipper (*Paphiopedilum*): IR expansion, SSC contraction, and highly rearranged SSC regions. BMC Plant Biol. **21**(1): 248.

Huang, Y.L., Oppong, M.B., Guo, Y., Wang, L.Z., Fang, S.M., Deng, Y.R. and Gao, X.M. 2019. The Oleaceae family: A source of secoiridoids with multiple biological activities. Fitoterapia **136**: 104155.

Jin, J.J., Yu, W.B., Yang, J.B., Song, Y., DePamphilis, C.W., Yi, T.S. and Li, D.Z. 2020. GetOrganelle: A fast and versatile toolkit for accurate *de novo* assembly of organelle genomes. Genome Biol. **21**(241): 1–31.

Katoh, K. and Standley, D.M. 2013. MAFFT multiple sequence alignment software version 7: Improvements in performance and usability. Mol. Biol. Evol. **30**(4): 772–780.

Kumar, S., Stecher, G., Suleski, M. and Hedges, S.B. 2017. TimeTree: A resource for timelines, timetrees, and divergence times. Mol. Biol. Evol. **34**(7): 1812–1819.

Kurtz, S., Choudhuri, J.V., Ohlebusch, E., Schleiermacher, C., Stoye, J. and Giegerich, R. 2001. REPuter: The manifold applications of repeat analysis on a genomic scale. Nucleic Acids Res. **29**(22): 4633–4642.

Li, X., Yang, Y., Henry, R.J., Rossetto, M., Wang, Y. and Chen, S. 2015. Plant DNA barcoding: From gene to genome. Biol. Rev. **90**(1): 157–166.

Librado, P. and Rozas, J. 2009. DnaSP v5: A software for comprehensive analysis of DNA polymorphism data. Bioinform. **25**(11): 1451–1452.

Liu, S., Ni, Y., Li, J., Zhang, X., Yang, H., Chen, H. and Liu, C. 2023. CPGView: A package for visualizing detailed chloroplast genome structures. Mol. Ecol. Resour. **23**(3): 694–704.

Macahig, R.A., Harinantenaina, L., Matsunami, K., Otsuka, H., Takeda, Y. and Shinzato, T. 2010. Secoiridoid and iridoid glucosides from the leaves of *Fraxinus griffithii*. J. Nat. Med. **64**: 1–8.

Okonechnikov, K., Golosova, O., Fursov, M. and Ugene Team. 2012. Unipro UGENE: A unified bioinformatics toolkit. Bioinform. **28**(8): 1166–1167.

Park, J., Xi, H. and Oh, S.H. 2020. Comparative chloroplast genomics and phylogenetic analysis of the *Viburnum dilatatum* complex (Adoxaceae) in Korea. Korean J Plant Taxon. **50**(1): 8–16.

Rahman, M.O. 2009. *Fraxinus griffithii* C.B. Clarke. *In*: Ahmed, Z.U., Hassan, M.A., Begum, Z.N.T., Khondker, M., Kabir, S.M.H., Ahmad, M., Ahmed, A.T.A., Rahman, A.K.A. and Haque, E.U. (Eds). Encyclopedia of Flora and Fauna of Bangladesh, Vol. **9**. Angiosperm: Dicotyledons (Magnoliaceae – Punicaceae). Asiatic Society of Bangladesh, Dhaka, pp. 323-324.

Shi, L., Chen, H., Jiang, M., Wang, L., Wu, X., Huang, L. and Liu, C. 2019. CPGAVAS2, an integrated plastome sequence annotator and analyzer. Nucleic Acids Res. **47**(W1): W65–W73.

Tamura, K., Stecher, G. and Kumar, S. 2021. MEGA11: Molecular evolutionary genetics analysis version 11. Mol. Biol. Evol. **38**(7): 3022–3027.

Wu, Y., Liu, F., Yang, D.G., Li, W., Zhou, X.J., Pei, X.Y., Liu, Y.G., He, K.L., Zhang, W.S., Ren, Z.Y., Zhou, K.H., Ma, X.F. and Li, Z.H. 2018. Comparative chloroplast genomics of *Gossypium species*: Insights into repeat sequence variations and phylogeny. Front. Plant Sci. **9**: 376.

Xiao, J. and Bai, W. 2019. Bioactive phytochemicals. Crit. Rev. Food Sci. Nutr. **59**(6): 827–829.

Yi, X., Li, M., Chen, L. and Wang, X. 2019. The complete chloroplast genome of *Fraxinus pennsylvanica* (Oleaceae). Mitochon. DNA Part B. **4**(1): 1932–1933.

Zhang, L., Wang, S., Su, C., Harris, A.J., Zhao, L., Su, N., Wang, J.R., Duan, L. and Chang, Z.Y. 2021b. Comparative chloroplast genomics and phylogenetic analysis of *Zygophyllum* (Zygophyllaceae) of China. Front. Plant Sci. **12**: 723622.

Zhang, X.F., Landis, J.B., Wang, H.X., Zhu, Z.X. and Wang, H.F. 2021a. Comparative analysis of chloroplast genome structure and molecular dating in Myrtales. BMC Plant Biol. **21**(1): 219.

Zheng, S., Poczai, P., Hyvönen, J., Tang, J. and Amiryousefi, A. 2020. Chloroplot: An online program for the versatile plotting of organelle genomes. Front. Genet. **11**: 576124.

(Manuscript received on 20 January 2025; revised on 3 June 2025)